Novel Hybrid RIS Architectures and Beamforming Optimization for Energy-Efficient Multi-User MISO

Konstantinos Ntougias, *Member, IEEE* and Ioannis Krikidis, *Fellow, IEEE*

***Abstract*—In this work, we introduce novel hybrid reflecting intelligent surface (RIS) architectures where at least one reflecting sub-surface (RS) resembles a sub-connected RIS. Next, assuming a multiple-input single-output broadcasting system where the base station (BS) is aided by a hybrid RIS adopting either one of the proposed structures or the fully-connected active/passive design, we jointly optimize the transmit precoding and reflect beamforming schemes to maximize the energy efficiency subject to the power consumption constraints of the BS and any active RS. We develop efficient, low-complexity iterative algorithms based on the Fractional Programming, Block Coordinate Descent, Lagrange multipliers, and Majorization-Minimization methods to tackle these challenging non-convex optimization problems and obtain closed-form expressions of the optimal solutions. We also derive the necessary conditions for feasible allocation of RIS elements. Numerical evaluations unveil the performance gains of the proposed designs over benchmarks and provide insights.**

***Index Terms*—Sub-connected active RIS, hybrid active/passive RIS, hybrid active RIS, energy efficiency, optimization.**

I. Introduction

The emerging reflecting intelligent surface (RIS) technology employs reflect beamforming (RB) to boost the performance of wireless communication systems [1]–[4]. However, the double path loss over the RIS-cascaded channels from the base station (BS) to the users significantly deteriorates the capacity gain when the respective direct channels are strong.

Fully-connected (FC) active RIS addresses this issue by integrating a reflect-type power amplifier (PA) into each reflecting element (RE). This RIS variant outperforms its *passive* counterpart under the same total power consumption (TPC) budget [5]–[8]. *Sub-connected (SC) active* RIS substantially reduces the TPC at the cost of only a slight capacity degradation, by forming disjoint RIS partitions and letting the REs within each one to share a common PA [9]. A hybrid FC-active/passive RIS design introduced in [10], to combine the capacity gains and TPC savings of these fundamental RIS architectures. As shown in that work, smaller TPC budgets and stronger links favor the deployment of active REs.

Motivated by [9], [10] and the urge to reduce the power consumption and carbon footprint of wireless networks in view of their extreme densification and the climate change [11], we introduce novel hybrid RIS architectures that employ the SC-active structure. Next, assuming perfect channel knowledge, we jointly optimize the transmit precoding (TP) and RB schemes in a hybrid RIS-aided multiple-input single-output (MISO) broadcasting system where the RIS adopts either one of the proposed hybrid structures or the design presented in [10], such that the energy efficiency (EE) is maximized subject to the TPC constraints of the BS and any active reflecting sub-surface (RS). We tackle these challenging non-convex optimization problems by developing efficient iterative algorithms that result in analytical expressions of the optimal solutions. We also derive the necessary conditions for feasible REs allocation. Numerical simulation results unveil the performance gains of the developed TP/RB schemes over benchmarks and provide valuable insights.

The paper is structured as follows: Sec. II introduces the proposed hybrid RIS structures and the system model. Sec. III presents the formulation and solution of the considered optimization problems. Sec. IV is devoted to performance evaluation via numerical simulations. Sec. V provides our conclusions and dicusses future extensions of this work.

Notation: $\mathbf{x}$: a column vector; $\mathbf{X}$: a matrix; $\mathbb{B}^{N\times M}$: the set of binary $N \times M$ matrices; $|x|$, $\arg(x)$, and $\mathrm{Re}\{x\}$: the magnitude, argument, and real part, respectively, of the complex scalar x; $\|\mathbf{x}\|$: the Euclidean norm of $\mathbf{x}$; $\mathbf{X}^*$, $\mathbf{X}^T$, $\mathbf{X}^\dagger$, $\mathbf{X}^{-1}$, and $\|\mathbf{X}\|_F$: the complex conjugate, transpose, complex conjugate transpose, inverse, and Frobenius norm of $\mathbf{X}$, respectively; $\mathbf{X} = \mathrm{diag}(\mathbf{x})$: a diagonal matrix with main diagonal $\mathbf{x} = \mathrm{Diag}(\mathbf{X})$; $\mathbf{X} \succeq \mathbf{0}$: a positive semi-definite (PSD) matrix $\mathbf{X}$; $\mathbf{1}_N$: the $N \times 1$ all-ones vector; $\mathbf{I}_N$: the $N \times N$ identity matrix; $\otimes$ and $\odot$: the Kronecker and Hadamard (element-wise) matrix product, respectively; $\mathcal{CN}(\cdot,\cdot)$: the circularly symmetric complex Gaussian distribution.

II. Hybrid RIS Structures and System Model

The considered setup consists of a BS with M antennas, a hybrid RIS with N REs, and K single-antenna terminals, as shown in Fig. 1. The RIS consists of two RSs equipped with N_s REs each, $s \in \mathcal{S} \triangleq \{1,2\}$, such that $N_1 + N_2 = N$. We define the index sets of REs in RS s, $\mathcal{N}_s \triangleq \{1,\ldots,N_s\}$, and users, $\mathcal{K} \triangleq \{1,\ldots,K\}$.

The transmitted signal, $\mathbf{x} \in \mathbb{C}^M$, is given by $\mathbf{x} = \sum_{k\in\mathcal{K}} \mathbf{w}_k s_k$, where $\mathbf{w}_k \in \mathbb{C}^M$ and $s_k \sim \mathcal{CN}(0,1)$ denote the TP vector and data symbol, respectively, of user $k \in \mathcal{K}$. The transmit sum-power (TSP) of the BS is written as

$$P_t = \mathbb{E}\left\{\|\mathbf{x}\|^2\right\} = \sum_{k\in\mathcal{K}} \|\mathbf{w}_k\|^2 . \tag{1}$$

This work has received funding from the European Research Council through the EU's Horizon 2020 Research and Innovation Programme under Grant 819819 and from the Research and Innovation Foundation under Grant DUAL USE/0922/0031. The authors are with the Department of Electrical and Computer Engineering, University of Cyprus, 1678 Nicosia, Cyprus. (E-mail: {ntougias.konstantinos, krikidis}@ucy.ac.cy).

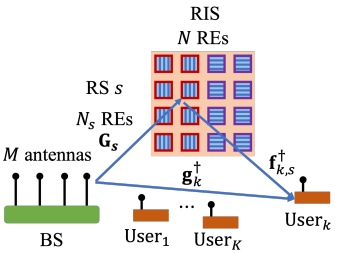

Fig. 1. System setup.

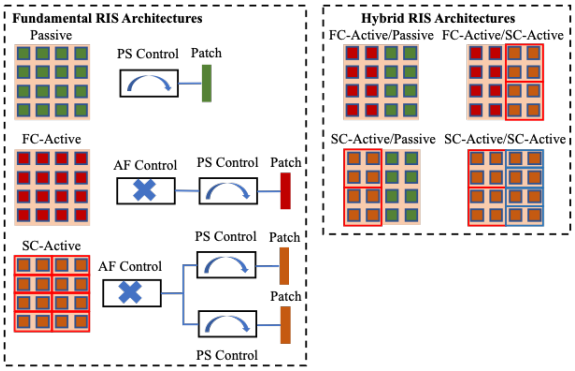

Fig. 2. Fundamental and hybrid RIS architectures.

The quasi-static, flat-fading baseband equivalent channels from the BS to user k, from the BS to RS s, and from RS s to user k are denoted by $\mathbf{g}_k^\dagger \in \mathbb{C}^M$, $\mathbf{G}_s \in \mathbb{C}^{N_s \times M}$, and $\mathbf{f}_{k,s}^\dagger \in \mathbb{C}^{N_s}$, respectively. The RB matrix of RS s is denoted by $\mathbf{\Phi}_s \in \mathbb{C}^{N_s \times N_s}$. The effective baseband equivalent channel from the BS to user k through RS s, $\mathbf{h}_{k,s}^\dagger \in \mathbb{C}^M$, is defined as $\mathbf{h}_{k,s}^\dagger \triangleq \mathbf{g}_k^\dagger + \mathbf{f}_{k,s}^\dagger \mathbf{\Phi}_s \mathbf{G}_s$.

We consider two families of hybrid RIS designs, namely, active/passive RIS architectures, consisting of the FC-active/passive and SC-active/passive RIS structures, and hybrid active RIS implementations, which include the FC-active/SC-active and hybrid SC-active RIS variants, as illustrated in Fig. 2. Consequently, each RS resembles the passive, FC-active, or SC-active architecture, which are depicted in Fig. 2. We respectively have for these RS structures:

$$\mathbf{\Phi}_s = \text{diag}\left(e^{j\theta_{1,s}}, \ldots, e^{j\theta_{N_s,s}}\right) \triangleq \mathbf{\Theta}_s, \tag{2a}$$

$$\mathbf{\Phi}_s = \text{diag}\left(\alpha_{1,s}e^{j\theta_{1,s}}, \ldots, \alpha_{N_s,s}e^{j\theta_{N_s,s}}\right) \triangleq \mathbf{\Theta}_s\mathbf{A}_s, \tag{2b}$$

$$\mathbf{\Phi}_s = \mathbf{\Theta}_s \,\text{diag}\left(\mathbf{\Gamma}_s\widetilde{\boldsymbol{\alpha}}_s\right), \tag{2c}$$

where we assumed that the SC-active RS has L_s disjoint partitions with $T_s = N_s/L_s$ REs each. We define the index set of these partitions as $\mathcal{L}_s \triangleq \{1, \ldots, L_s\}$. In Eq. (2), $\theta_{n,s} \in [0, 2\pi)$ and $\alpha_{n,s} \geq 0$, $n \in \mathcal{N}_s$, represent the phase shift (PS) and amplification factor (AF), respectively, of the n-th RE in RS s, $\mathbf{\Theta}_s \in \mathbb{C}^{N_s \times N_s}$ is the PSs matrix, $\mathbf{A}_s \in \mathbb{R}_+^{N_s \times N_s}$ is the AFs matrix defined as $\mathbf{A}_s \triangleq \text{diag}\left(\alpha_{1,s}, \ldots, \alpha_{N_s,s}\right)$, $\widetilde{\boldsymbol{\alpha}}_s \in \mathbb{R}_+^{L_s}$ is the AFs vector for the SC-active RS case defined as $\widetilde{\boldsymbol{\alpha}}_s \triangleq [\widetilde{\alpha}_{1,s}, \ldots, \widetilde{\alpha}_{L_s,s}]^T$, with $\widetilde{\alpha}_{l,s} \geq 0$, $l \in \mathcal{L}_s$, denoting the AF of the l-th partition, and $\mathbf{\Gamma}_s \in \mathbb{B}^{N_s \times L_s}$ stands for the coupling matrix defined as $\mathbf{\Gamma}_s \triangleq \mathbf{I}_{L_s} \otimes \mathbf{1}_{T_s}$. FC-active RS is a special case of SC-active RS with $T_s = 1$ (i.e., $L_s = N_s$) and passive RS is a special case of FC-active RS with $\mathbf{A}_s = \mathbf{I}_{N_s}$ (i.e., $\alpha_{n,s} = 1$, $\forall n \in \mathcal{N}_s$).

If RS s is active, then the amplified and reflected signal, $\mathbf{t}_s \in \mathbb{C}^{N_s}$, is written as $\mathbf{t}_s = \mathbf{\Phi}_s\left(\mathbf{r}_s + \mathbf{z}_s\right)$, where $\mathbf{r}_s \in \mathbb{C}^{N_s}$ denotes the incident signal given by $\mathbf{r}_s = \mathbf{G}_s\mathbf{x}$ and $\mathbf{z}_s \sim \mathcal{CN}\left(\mathbf{0}_{N_s}, \delta_s^2\mathbf{I}_{N_s}\right)$ represents the amplification noise. The TSP of this RS is expressed as

$$P_{r,s} = \mathbb{E}\left\{\|\mathbf{t}_s\|^2\right\} = \sum_{k\in\mathcal{K}} \|\mathbf{\Phi}_s\mathbf{G}_s\mathbf{w}_k\|^2 + \delta_s^2\|\mathbf{\Phi}_s\|_F^2. \tag{3}$$

The TPC of the BS, the terminals, and RS s is written as

$$P_{\text{BS}} = \xi^{-1}P_t + W_{\text{BS}}, \; P_{\text{UE}} = \sum_{k\in\mathcal{K}} W_{\text{UE}}, \tag{4a}$$

$$P_s = N_s P_{\text{PS}}, \; \text{(Passive RS)} \tag{4b}$$

$$P_s = \zeta_s^{-1}P_{r,s} + W_{r,s}, \; \text{(Active RS)} \tag{4c}$$

where W_{BS}, $W_{r,s}$, and W_{UE} refer to the static power consumption of the BS, active RS s, and each user equipment (UE), respectively, which is attributed to their hardware, $\xi \in (0,1)$ and $\zeta_s \in (0,1)$ represent the energy efficiency of the amplification hardware installed in the BS and active RS s, respectively, and P_{PS} denotes the power consumption of the PS control circuit of each RE. We have:

$$W_{r,s} = N_s\left(P_{\text{PS}} + P_{\text{DC}}\right), \; \text{(FC-active RS)} \tag{5a}$$

$$W_{r,s} = N_s P_{\text{PS}} + \left(N_s/T_s\right)P_{\text{DC}}, \; \text{(SC-active RS)} \tag{5b}$$

where P_{DC} denotes the direct current (DC) bias of each PA. The TPC constraint of the BS and active RS s is given by $P_{\text{BS}} \leq P_{\text{BS}}^{\max}$ and $P_s \leq P_s^{\max}$, respectively, where $P_{\text{BS}}^{\max} > 0$ and $P_s^{\max} > 0$ denote the corresponding TPC budgets. By denoting $P_{\text{RIS}} = \sum_{s\in\mathcal{S}} P_s$ and $\widetilde{P} \triangleq P_{\text{BS}} + P_{\text{UE}}$, we can write the TPC of the system as $P = \widetilde{P} + P_{\text{RIS}}$.

The rate of user k, R_k, and the sum-rate (SR), R, are given by $R_k = \log_2\left(1+\gamma_k\right)$ and $R = \sum_{k\in\mathcal{K}} R_k$, respectively, where $\gamma_k > 0$ is the signal-to-interference-plus-noise-ratio (SINR) of user k. The EE of the system is written as $\eta = R/P$.

The received signal at user k through RS s in the case where this RS is passive, ignoring the thermal noise, is written as

$$y_{k,s} = \mathbf{h}_{k,s}^\dagger\mathbf{x} = \underbrace{\mathbf{h}_{k,s}^\dagger\mathbf{w}_k s_k}_{\text{useful signal}} + \underbrace{\mathbf{h}_{k,s}^\dagger \sum_{i\in\mathcal{K}\setminus\{k\}} \mathbf{w}_i s_i}_{\text{multi-user interference}}. \tag{6}$$

If RS is active, $y_{k,s} = \mathbf{g}_k^\dagger\mathbf{x} + \mathbf{f}_{k,s}^\dagger\mathbf{t}_s = \mathbf{h}_{k,s}^\dagger\mathbf{x} + \mathbf{f}_{k,s}^\dagger\mathbf{\Phi}_s\mathbf{z}_s$, i.e.,

$$y_{k,s} = \underbrace{\mathbf{h}_{k,s}^\dagger\mathbf{w}_k s_k}_{\text{useful signal}} + \underbrace{\mathbf{h}_{k,s}^\dagger \sum_{i\in\mathcal{K}\setminus\{k\}} \mathbf{w}_i s_i}_{\text{multi-user interference}} + \underbrace{\mathbf{f}_{k,s}^\dagger\mathbf{\Phi}_s\mathbf{z}_s}_{\text{amplification noise}}. \tag{7}$$

The composite received signal at user k is expressed as $y_k = \sum_{s\in\mathcal{S}} y_{k,s} + n_k$, where $n_k \sim \mathcal{CN}\left(0, \sigma_k^2\right)$ denotes the additive white Gaussian noise (AWGN).

Hybrid Active/Passive RIS: When the RIS adopts the FC-active/passive design presented in [10] or the proposed SC-active/passive one, the received signal at user k is given by

$$y_k = \sum_{s\in\mathcal{S}} \mathbf{h}_{k,s}^\dagger \mathbf{w}_k s_k + \sum_{s\in\mathcal{S}} \mathbf{h}_{k,s}^\dagger \sum_{i\in\mathcal{K}\setminus\{k\}} \mathbf{w}_i s_i + \mathbf{f}_{k,1}^\dagger \mathbf{\Phi}_1 \mathbf{z}_1 + n_k. \tag{8}$$

Hence, the SINR of this user is written as

$$\gamma_k = \frac{\sum\limits_{s\in\mathcal{S}} \left\| \mathbf{h}_{k,s}^\dagger \mathbf{w}_k \right\|^2}{\sum\limits_{s\in\mathcal{S}} \sum\limits_{i\in\mathcal{K}\setminus\{k\}} \left\| \mathbf{h}_{k,s}^\dagger \mathbf{w}_i \right\|^2 + \delta_1^2 \left\| \mathbf{f}_{k,1}^\dagger \mathbf{\Phi}_1 \right\|^2 + \sigma_k^2}. \tag{9}$$

Hybrid Active RIS: When the RIS adopts the proposed FC-/SC-active structure or consists of two SC-active RSs with different partitioning, the received signal at user k is given by

$$y_k = \sum_{s\in\mathcal{S}} \mathbf{h}_{k,s}^\dagger \mathbf{w}_k s_k + \sum_{s\in\mathcal{S}} \mathbf{h}_{k,s}^\dagger \sum_{i\in\mathcal{K}\setminus\{k\}} \mathbf{w}_i s_i + \sum_{s\in\mathcal{S}} \mathbf{f}_{k,s}^\dagger \mathbf{\Phi}_s \mathbf{z}_s + n_k. \tag{10}$$

Therefore, the SINR of this user is expressed as

$$\gamma_k = \frac{\sum\limits_{s\in\mathcal{S}} \left\| \mathbf{h}_{k,s}^\dagger \mathbf{w}_k \right\|^2}{\sum\limits_{s\in\mathcal{S}} \left(\sum\limits_{i\in\mathcal{K}\setminus\{k\}} \left\| \mathbf{h}_{k,s}^\dagger \mathbf{w}_i \right\|^2 + \delta_s^2 \left\| \mathbf{f}_{k,s}^\dagger \mathbf{\Phi}_s \right\|^2 \right) + \sigma_k^2}. \tag{11}$$

III. Problem Formulation and Solutions

A. Hybrid Active/Passive RIS

In the hybrid active/passive RIS case, the optimization problem of interest is mathematically formulated as follows:

$$\text{(P1):} \max_{\mathbf{w},\{\boldsymbol{\phi}_s\}} \eta = \frac{R}{P} = \frac{\sum\limits_{k\in\mathcal{K}} \log_2(1+\gamma_k)}{\widetilde{P} + P_1 + N_2 P_{\text{PS}}} \tag{12a}$$

$$\text{s.t.} \quad \text{C1: } P_{\text{BS}} = \xi^{-1} \sum_{k\in\mathcal{K}} \|\mathbf{w}_k\|^2 + W_{\text{BS}} \le P_{\text{BS}}^{\max}, \tag{12b}$$

$$\text{C2: } P_1 = \zeta_1^{-1} \left(\sum_{k\in\mathcal{K}} \|\mathbf{\Phi}_1 \mathbf{G}_1 \mathbf{w}_k\|^2 + \delta_1^2 \|\mathbf{\Phi}_1\|_F^2 \right) + W_{r,1} \le P_1^{\max}, \tag{12c}$$

$$\text{C3: } |[\boldsymbol{\phi}_2]_n| = 1, \ \forall n \in \mathcal{N}_2, \tag{12d}$$

where we have respectively defined $\mathbf{w} \in \mathbb{C}^{KM}$ and $\boldsymbol{\phi}_s \in \mathbb{C}^{N_s}$ as $\mathbf{w} \triangleq \left[\mathbf{w}_1^T, \ldots, \mathbf{w}_K^T\right]^T$ and $\boldsymbol{\phi}_s \triangleq \text{Diag}\left(\mathbf{\Phi}_s^*\right)$, γ_k is given by Eq. (9), and $W_{r,1}$ is given by Eq. (5a) or Eq. (5b) if RS1 resembles an FC-active or an SC-active RIS, respectively.

(P1) is a challenging non-convex optimization problem, due to the fractional form of the objective function (OF), the intrinsic coupling of the decision variables in the OF and the constraints, and the unit modulus constraints (UMC) C3.

1) Fractional Programming: We adopt Fractional Programming (FP) to transform the fractional OF in problem (P1) [9]. Specifically, by utilizing Dinkelbach's algorithm, we convert the OF to $f(\mathbf{w}, \boldsymbol{\phi}) = R - \eta P$, where we have defined $\boldsymbol{\phi} \in \mathbb{C}^N$ as $\boldsymbol{\phi} \triangleq \left[\boldsymbol{\phi}_1^T, \boldsymbol{\phi}_2^T\right]^T$ for convenience. This new OF is still non-convex; nonetheless, by applying the Lagrangian dual transform (LDT) and the quadratic transform (QT) [12], we can equivalently recast (P1) as:

$$\text{(P2):} \max_{\mathbf{w},\boldsymbol{\phi},\boldsymbol{\mu},\boldsymbol{\nu}} g(\mathbf{w}, \boldsymbol{\phi}, \boldsymbol{\mu}, \boldsymbol{\nu}) \ \text{ s.t. C1–C3,} \tag{13}$$

where $\boldsymbol{\mu} \in \mathbb{C}^K$ and $\boldsymbol{\nu} \in \mathbb{C}^K$ are auxiliary variables and

$$g(\mathbf{w}, \boldsymbol{\phi}, \boldsymbol{\mu}, \boldsymbol{\nu}) = -\eta P + \sum_{k\in\mathcal{K}} \left[\ln(1+\mu_k) - \mu_k + 2\sqrt{1+\mu_k} \sum_{s\in\mathcal{S}} \text{Re}\left\{ \nu_k^* \mathbf{h}_{k,s}^\dagger \mathbf{w}_k \right\} - |\nu_k|^2 \left(\sum_{i\in\mathcal{K}} \sum_{s\in\mathcal{S}} \left| \mathbf{h}_{k,s}^\dagger \mathbf{w}_i \right|^2 + \left\| \mathbf{f}_{k,1}^\dagger \mathbf{\Phi}_1 \right\|^2 \delta_1^2 + \sigma_k^2 \right) \right]. \tag{14}$$

Next, we develop a Block Coordinate Ascent (BCA) algorithm to alternately optimize each variable with the others being fixed in each iteration until convergence.

2) Optimal Auxiliary Variables: By setting $\partial g / \partial \mu_k = 0$ and $\partial g / \partial \nu_k = 0$ with fixed $(\mathbf{w}, \boldsymbol{\phi}, \boldsymbol{\nu})$ and $(\mathbf{w}, \boldsymbol{\phi}, \boldsymbol{\mu})$, $\forall k \in \mathcal{K}$, and defining $\rho_k \triangleq \sum_{s\in\mathcal{S}} \text{Re}\left\{ \nu_k^* \mathbf{h}_{k,s}^\dagger \mathbf{w}_k \right\}$, we obtain:

$$\mu_k^\star = \frac{\rho_k}{2} \left(\rho_k + \sqrt{\rho_k^2 + 4} \right), \tag{15a}$$

$$\nu_k^\star = \frac{\sqrt{1+\mu_k} \sum\limits_{s\in\mathcal{S}} \mathbf{h}_{k,s}^\dagger \mathbf{w}_k}{\sum\limits_{i\in\mathcal{K}} \sum\limits_{s\in\mathcal{S}} \left| \mathbf{h}_{k,s}^\dagger \mathbf{w}_i \right|^2 + \left\| \mathbf{f}_{k,1}^\dagger \mathbf{\Phi}_1 \right\|^2 \delta_1^2 + \sigma_k^2}. \tag{15b}$$

3) Optimal Transmit Precoding: We note in Eqs. (12b) and (12c) that the TSP budget of the BS and RS1 equal

$$\widetilde{P}_{\text{BS}}^{\max} = \xi \left(P_{\text{BS}}^{\max} - W_{\text{BS}} \right), \tag{16a}$$

$$\widetilde{P}_1^{\max} = \zeta_1 \left(P_1^{\max} - W_{r,1} \right). \tag{16b}$$

Let us define $\mathbf{u}_k \in \mathbb{C}^M$, $\mathbf{u} \in \mathbb{C}^{KM}$, $\mathbf{S} \in \mathbb{C}^{KM\times KM}$, and $\mathbf{T} \in \mathbb{C}^{KM\times KM}$ as

$$\mathbf{u}_k \triangleq \sum_{s\in\mathcal{S}} 2\sqrt{1+\mu_k} \nu_k \mathbf{h}_{k,s}, \ \mathbf{u} \triangleq \left[\mathbf{u}_1^T, \ldots, \mathbf{u}_K^T\right]^T, \tag{17a}$$

$$\mathbf{S} \triangleq \mathbf{I}_K \otimes \left(\eta \xi^{-1} \mathbf{I}_M + \eta \zeta_1^{-1} \mathbf{G}_1^\dagger \mathbf{\Phi}_1^\dagger \mathbf{\Phi}_1 \mathbf{G}_1 + \sum_{k\in\mathcal{K}} \sum_{s\in\mathcal{S}} |\nu_k|^2 \mathbf{h}_{k,s} \mathbf{h}_{k,s}^\dagger \right), \tag{17b}$$

$$\mathbf{T} \triangleq \mathbf{I}_K \otimes \left(\mathbf{G}_1^\dagger \mathbf{\Phi}_1^\dagger \mathbf{\Phi}_1 \mathbf{G}_1 \right). \tag{17c}$$

Hence, with fixed $(\boldsymbol{\phi}, \boldsymbol{\mu}, \boldsymbol{\nu})$, the TP optimization sub-problem can be formulated as follows:

$$\text{(P3):} \max_{\mathbf{w}} \text{Re}\left\{ \mathbf{u}^\dagger \mathbf{w} \right\} - \mathbf{w}^\dagger \mathbf{S} \mathbf{w} \tag{18a}$$

$$\text{s.t.} \quad \text{C1: } \mathbf{w}^\dagger \mathbf{w} \le \widetilde{P}_{\text{BS}}^{\max}, \tag{18b}$$

$$\text{C2: } \mathbf{w}^\dagger \mathbf{T} \mathbf{w} \le \widetilde{P}_1^{\max} - \delta_1^2 \|\mathbf{\Phi}_1\|_F^2. \tag{18c}$$

(P3) is a standard convex Quadratically Constrained Quadratic Program (QCQP), which can be solved by using the Lagrange multiplier method to obtain [8]

$$\mathbf{w}^{\star} = \frac{1}{2}(\mathbf{S} + \lambda_1 \mathbf{I}_{KM} + \lambda_2 \mathbf{T})^{-1}\mathbf{u}, \tag{19}$$

where the Lagrange multipliers corresponding to the constraints C1 and C2, λ_1 and λ_2, are optimized via grid search.

4) Optimal RIS Beamforming: Let $\alpha_{k,i} \triangleq \mathbf{g}_k^{\dagger}\mathbf{w}_i$. We define $\boldsymbol{\beta}_{s,i} \in \mathbb{C}^N$ as $\boldsymbol{\beta}_{s,i} \triangleq \mathbf{G}_s\mathbf{w}_i$. Then, $\mathbf{h}_{k,s}^{\dagger}\mathbf{w}_i \triangleq \alpha_{k,i} + \mathbf{f}_{k,s}^{\dagger}\operatorname{diag}(\boldsymbol{\beta}_{s,i})\boldsymbol{\phi}_s$. We also define $\boldsymbol{\upsilon}_s \in \mathbb{C}^{N_s}$, $\mathbf{Q}_s \in \mathbb{C}^{N_s \times N_s}$, $\mathbf{Q}_s \succeq \mathbf{0}$, and $\mathbf{R} \in \mathbb{C}^{N_1 \times N_1}$ as

$$\boldsymbol{\upsilon}_s \triangleq \sum_{k\in\mathcal{K}} \operatorname{diag}\left(\mathbf{f}_{k,s}^{\dagger}\right) \times \left(2\sqrt{1+\mu_k}\nu_k^{*}\boldsymbol{\beta}_{s,k} - |\nu_k|^2 \sum_{i\in\mathcal{K}} \alpha_{k,i}^{*}\boldsymbol{\beta}_{s,i}\right), \tag{20a}$$

$$\mathbf{Q}_1 \triangleq \sum_{k\in\mathcal{K}} \Big(|\nu_k|^2 \delta_1^2 \operatorname{diag}\left(\mathbf{f}_{k,1} \odot \mathbf{f}_{k,1}^{*}\right) + \eta\zeta_1 \operatorname{diag}\left(\boldsymbol{\beta}_{1,k} \odot \boldsymbol{\beta}_{1,k}^{*}\right)\Big) + \sum_{k\in\mathcal{K}} |\nu_k|^2 \sum_{i\in\mathcal{K}} \operatorname{diag}\left(\boldsymbol{\beta}_{1,i}^{*}\right) \mathbf{f}_{k,1}\mathbf{f}_{k,1}^{\dagger} \operatorname{diag}\left(\boldsymbol{\beta}_{1,i}\right) + \eta\zeta_1\delta_1^2\mathbf{I}_{N_1}, \tag{20b}$$

$$\mathbf{Q}_2 \triangleq \sum_{k\in\mathcal{K}} |\nu_k|^2 \sum_{i\in\mathcal{K}} \operatorname{diag}\left(\boldsymbol{\beta}_{2,i}^{*}\right) \mathbf{f}_{k,2}\mathbf{f}_{k,2}^{\dagger} \operatorname{diag}\left(\boldsymbol{\beta}_{2,i}\right), \tag{20c}$$

$$\mathbf{R} \triangleq \sum_{k\in\mathcal{K}} \operatorname{diag}\left(\boldsymbol{\beta}_{1,k} \odot \boldsymbol{\beta}_{1,k}^{*}\right) + \delta_1^2\mathbf{I}_{N_1}. \tag{20d}$$

Hence, by fixing $(\mathbf{w}, \boldsymbol{\phi}_2, \boldsymbol{\mu}, \boldsymbol{\nu})$ and dropping the respective constant terms from the OF, we obtain the following sub-problem for optimizing $\boldsymbol{\phi}_1$:

$$\text{(P4-A)}: \max_{\boldsymbol{\phi}_1} \operatorname{Re}\left\{\boldsymbol{\phi}_1^{\dagger}\boldsymbol{\upsilon}_1\right\} - \boldsymbol{\phi}_1^{\dagger}\mathbf{Q}_1\boldsymbol{\phi}_1 \text{ s.t. C2: } \boldsymbol{\phi}_1^{\dagger}\mathbf{R}\boldsymbol{\phi}_1 \le \widetilde{P}_1^{\max}. \tag{21}$$

We use the Lagrangian multipliers method to tackle this standard QCQP and obtain a closed-form expression of $\boldsymbol{\phi}_1^{\star}$:

$$\boldsymbol{\phi}_1^{\star} = \frac{1}{2}\left(\mathbf{Q}_1 + \varpi\mathbf{R}\right)^{-1}\boldsymbol{\upsilon}_1, \tag{22}$$

where the Lagrange multiplier associated with C2, ϖ, is optimized via binary search. The optimal PSs matrix is given by $\boldsymbol{\Theta}_1^{\star} = \operatorname{diag}\left(e^{j\arg((\boldsymbol{\phi}_1^{\star})^{*})}\right)$ [9]. When RS1 resembles an FC-active or SC-active RIS, then $[\mathbf{A}_1^{\star}]_{n,n} = |[\boldsymbol{\phi}_1^{\star}]_n|$ or $\boldsymbol{\alpha}_1^{\star} = \boldsymbol{\Gamma}_1^{+}\operatorname{diag}\left(e^{-j\arg((\boldsymbol{\phi}_1^{\star})^{*})}\right)(\boldsymbol{\phi}_1^{\star})^{*}$, respectively [9].

With fixed $\boldsymbol{\phi}_1$, we form the minimization sub-problem:

$$\text{(P4-B)}: \min_{\boldsymbol{\phi}_2} h(\boldsymbol{\phi}_2) = \boldsymbol{\phi}_2^{\dagger}\mathbf{Q}_2\boldsymbol{\phi}_2 - \operatorname{Re}\left\{\boldsymbol{\phi}_2^{\dagger}\boldsymbol{\upsilon}_2\right\} \text{ s.t. C3.} \tag{23}$$

We apply the Majorization-Minimization (MM) method to handle the UMCs C3. Specifically, for any given solution $\boldsymbol{\phi}_2^t$ at the t-th iteration of the MM algorithm and any feasible $\boldsymbol{\phi}_2$, we have [13]

$$\boldsymbol{\phi}_2^{\dagger}\mathbf{Q}_2\boldsymbol{\phi}_2 \le \boldsymbol{\phi}_2^{\dagger}\mathbf{X}\boldsymbol{\phi}_2 - 2\operatorname{Re}\left\{\boldsymbol{\phi}_2^{\dagger}\left(\mathbf{X} - \mathbf{Q}_2\right)\boldsymbol{\phi}_2^t\right\} + \left(\boldsymbol{\phi}_2^t\right)^{\dagger}\left(\mathbf{X} - \mathbf{Q}_2\right)\boldsymbol{\phi}_2^t \triangleq y\left(\boldsymbol{\phi}_2|\boldsymbol{\phi}_2^t\right), \tag{24}$$

where $\mathbf{X} = \lambda_{\max}\mathbf{I}_{N_2}$, $\lambda_{\max}$ denotes the maximum eigenvalue of $\mathbf{Q}_2$, and $\mathbf{X} \succeq \mathbf{Q}_2$, $\mathbf{X} \in \mathbb{R}_{+}^{N_2 \times N_2}$. We replace the OF in problem (P4-B) by a surrogate OF, which is defined as $z\left(\boldsymbol{\phi}_2|\boldsymbol{\phi}_2^t\right) \triangleq y\left(\boldsymbol{\phi}_2|\boldsymbol{\phi}_2^t\right) - \operatorname{Re}\left\{\boldsymbol{\phi}_2^{\dagger}\boldsymbol{\upsilon}_2\right\}$. The new OF represents an upper bound of the original one and coincides with it at point $\boldsymbol{\phi}_2^t$. By removing the constant terms in this new OF, such as $\boldsymbol{\phi}_2^{\dagger}\mathbf{X}\boldsymbol{\phi} = N_2\lambda_{\max}$, we obtain:

$$\text{(P4-C)}: \max_{\boldsymbol{\phi}_2} \operatorname{Re}\left\{\boldsymbol{\phi}_2^{\dagger}\mathbf{q}^t\right\} \text{ s.t. C3,} \tag{25}$$

where $\mathbf{q}^t \in \mathbb{C}^{N_2}$ is defined as $\mathbf{q}^t \triangleq \left(\mathbf{X} - \mathbf{Q}_2\right)\boldsymbol{\phi}_2^t + \boldsymbol{\upsilon_2}$ [13]. The optimal solution of problem (P4-C) is given by [13]

$$\boldsymbol{\phi}_2^{t+1} = e^{j\arg\left(\mathbf{q}^t\right)}. \tag{26}$$

B. Hybrid Active RIS

In the hybrid active RIS case, the optimization problem of interest is formulated as follows:

$$\text{(P5)}: \max_{\mathbf{w},\{\boldsymbol{\phi}_s\}} \eta = \frac{R}{P} = \frac{\sum_{k\in\mathcal{K}} \log_2\left(1+\gamma_k\right)}{\widetilde{P} + \sum_{s\in\mathcal{S}} P_s} \tag{27a}$$

$$\text{s.t.} \quad \text{C5: } P_{\text{BS}} = \xi^{-1}\sum_{k\in\mathcal{K}} \|\mathbf{w}_k\|^2 + W_{\text{BS}} \le P_{\text{BS}}^{\max}, \tag{27b}$$

$$\text{C6: } P_s = \zeta_s^{-1}\left(\sum_{k\in\mathcal{K}} \|\boldsymbol{\Phi}_s\mathbf{G}_s\mathbf{w}_k\|^2 + \delta_s^2\|\boldsymbol{\Phi}_s\|_F^2\right) + W_{r,s} \le P_s^{\max}, \forall s \in \mathcal{S}, \tag{27c}$$

where γ_k and $W_{r,2}$ are given by Eqs. (11) and (5b), respectively, whereas $W_{r,1}$ is given by either Eq. (5a) or Eq. (5b), depending on whether RS1 resembles an FC-active RIS or an SC-active one, respectively.

1) Fractional Programming: By using Dinkelbach's algorithm along with the LDT and QT [12], we can equivalently recast (P5) as:

$$\text{(P6)}: \max_{\mathbf{w},\boldsymbol{\phi},\boldsymbol{\mu}',\boldsymbol{\nu}'} g'\left(\mathbf{w},\boldsymbol{\phi},\boldsymbol{\mu}',\boldsymbol{\nu}'\right) \text{ s.t. C5, C6,} \tag{28}$$

where $\boldsymbol{\mu}' \in \mathbb{C}^K$ and $\boldsymbol{\nu}' \in \mathbb{C}^K$ are auxiliary variables and

$$g'\left(\mathbf{w},\boldsymbol{\phi},\boldsymbol{\mu}',\boldsymbol{\nu}'\right) = -\eta P + \sum_{k\in\mathcal{K}} \Big[\ln\left(1+\mu_k'\right) - \mu_k' + 2\sqrt{1+\mu_k'}\sum_{s\in\mathcal{S}} \operatorname{Re}\left\{\left(\nu_k'\right)^{*}\mathbf{h}_{k,s}^{\dagger}\mathbf{w}_k\right\} - |\nu_k'|^2\left(\sum_{i\in\mathcal{K}}\sum_{s\in\mathcal{S}}\left|\mathbf{h}_{k,s}^{\dagger}\mathbf{w}_i\right|^2 + \sum_{s\in\mathcal{S}}\left\|\mathbf{f}_{k,s}^{\dagger}\boldsymbol{\Phi}_s\right\|^2\delta_s^2 + \sigma_k^2\right)\Big]. \tag{29}$$

2) Optimal Auxiliary Variables: By setting $\partial g'/\partial\mu_k' = 0$ and $\partial g'/\partial\nu_k' = 0$ with fixed $(\mathbf{w},\boldsymbol{\phi},\boldsymbol{\nu}')$ and $(\mathbf{w},\boldsymbol{\phi},\boldsymbol{\mu}')$, $\forall k \in \mathcal{K}$, and defining $\rho_k' \triangleq \sum_{s\in\mathcal{S}} \operatorname{Re}\left\{\left(\nu_k'\right)^{*}\mathbf{h}_{k,s}^{\dagger}\mathbf{w}_k\right\}$, we obtain:

$$\nu_k'^{,\star} = \frac{\sqrt{1+\mu_k'}\sum_{s\in\mathcal{S}}\mathbf{h}_{k,s}^{\dagger}\mathbf{w}_k}{\sum_{i\in\mathcal{K}}\sum_{s\in\mathcal{S}}\left|\mathbf{h}_{k,s}^{\dagger}\mathbf{w}_i\right|^2 + \sum_{s\in\mathcal{S}}\left\|\mathbf{f}_{k,s}^{\dagger}\boldsymbol{\Phi}_s\right\|^2\delta_s^2 + \sigma_k^2}, \tag{30a}$$

$$\mu_k'^{,\star} = \frac{\rho_k'}{2}\left(\rho_k' + \sqrt{\left(\rho_k'\right)^2 + 4}\right). \tag{30b}$$

3) Optimal Transmit Precoding: From Eq. (27c),

$$\widetilde{P}_2^{\max} = \zeta_2 \left(P_2^{\max} - W_{r,2}\right). \tag{31}$$

We also set $\mathbf{T}_1 = \mathbf{T}$ and define $\mathbf{S}' \in \mathbb{C}^{KM\times KM}$ and $\mathbf{T}_2 \in \mathbb{C}^{KM\times KM}$ as

$$\mathbf{S}' \triangleq \mathbf{I}_K \otimes \Bigg(\eta\xi^{-1}\mathbf{I}_M + \sum_{s\in\mathcal{S}} \eta\zeta_s^{-1}\mathbf{G}_s^\dagger \mathbf{\Phi}_s^\dagger \mathbf{\Phi}_s \mathbf{G}_s + \sum_{k\in\mathcal{K}}\sum_{s\in\mathcal{S}} \left|\nu_k'\right|^2 \mathbf{h}_{k,s}\mathbf{h}_{k,s}^\dagger\Bigg), \tag{32a}$$

$$\mathbf{T}_2 \triangleq \mathbf{I}_K \otimes \left(\mathbf{G}_2^\dagger \mathbf{\Phi}_2^\dagger \mathbf{\Phi}_2 \mathbf{G}_2\right). \tag{32b}$$

Hence, with fixed $(\boldsymbol{\phi}, \boldsymbol{\mu}', \boldsymbol{\nu}')$, the TP optimization sub-problem can be formulated as follows:

$$\text{(P7):} \max_{\mathbf{w}} \mathrm{Re}\left\{\mathbf{u}^\dagger\mathbf{w}\right\} - \mathbf{w}^\dagger\mathbf{S}'\mathbf{w} \tag{33a}$$

$$\text{s.t.} \quad \text{C5: } \mathbf{w}^\dagger\mathbf{w} \le \widetilde{P}_{\text{BS}}^{\max}, \tag{33b}$$

$$\text{C6: } \mathbf{w}^\dagger\mathbf{T}_s\mathbf{w} \le \widetilde{P}_s^{\max} - \delta_s^2 \left\|\mathbf{\Phi}_s\right\|_F^2, \ \forall s \in \mathcal{S}. \tag{33c}$$

(P7) is a standard convex QCQP which can be solved by using the Lagrange multiplier method to obtain:

$$\mathbf{w}^\star = \frac{1}{2}(\mathbf{S}' + \lambda'\mathbf{I}_{KM} + \sum_{s\in\mathcal{S}} \psi_s\mathbf{T}_s)^{-1}\mathbf{u}, \tag{34}$$

where λ' and ψ_s represent the Lagrange multipliers that are associated with constraints C5 and C6, respectively, and are optimized via grid search.

4) Optimal RIS Beamforming: Let us define $\mathbf{Q}_s' \in \mathbb{C}^{N_s\times N_s}$ and $\mathbf{R}_s \in \mathbb{C}^{N_s\times N_s}$ as

$$\mathbf{Q}_s' \triangleq \sum_{k\in\mathcal{K}} \Big(\left|\nu_k'\right|^2 \delta_s^2 \,\mathrm{diag}\left(\mathbf{f}_{k,s}\odot\mathbf{f}_{k,s}^*\right) + \eta\zeta_s \,\mathrm{diag}\left(\boldsymbol{\beta}_{s,k}\odot\boldsymbol{\beta}_{s,k}^*\right)\Big) + \sum_{k\in\mathcal{K}} \left|\nu_k'\right|^2 \sum_{i\in\mathcal{K}} \mathrm{diag}\left(\boldsymbol{\beta}_{s,i}^*\right)\mathbf{f}_{k,s}\mathbf{f}_{k,s}^\dagger \,\mathrm{diag}\left(\boldsymbol{\beta}_{s,i}\right) + \eta\zeta_s\delta_s^2\mathbf{I}_{N_s}, \tag{35a}$$

$$\mathbf{R}_s \triangleq \sum_{k\in\mathcal{K}} \mathrm{diag}\left(\boldsymbol{\beta}_{s,k}\odot\boldsymbol{\beta}_{s,k}^*\right) + \delta_s^2\mathbf{I}_{N_s}. \tag{35b}$$

Hence, with fixed $(\mathbf{w}, \boldsymbol{\mu}', \boldsymbol{\nu}')$, we can formulate the RB optimization sub-problem as follows:

$$\text{(P8):} \max_{\boldsymbol{\phi}} \sum_{s\in\mathcal{S}} \left(\mathrm{Re}\left\{\boldsymbol{\phi}_s^\dagger\boldsymbol{\upsilon}_s\right\} - \boldsymbol{\phi}_s^\dagger\mathbf{Q}_s'\boldsymbol{\phi}_s\right) \tag{36a}$$

$$\text{s.t.} \quad \text{C6: } \boldsymbol{\phi}_s^\dagger\mathbf{R}_s\boldsymbol{\phi}_s \le \widetilde{P}_s^{\max}. \tag{36b}$$

Fixing $\boldsymbol{\phi}_2$ and solving for $\boldsymbol{\phi}_1$ or vice-versa, we formulate the standard convex QCQPs (P8-A) and (P8-B), respectively. By using the Lagrange multipliers method, we obtain:

$$\boldsymbol{\phi}_s^\star = \frac{1}{2}\left(\mathbf{Q}_s' + \varpi_s\mathbf{R}_s\right)^{-1}\boldsymbol{\upsilon}_s, \tag{37}$$

where ϖ_s represents the Lagrange multiplier associated with the constraints C6 with fixed $s = 1$ or $s = 2$ in each case, respectively, and is optimized via binary search.

C. Feasible Deployment of RIS Elements

The number of active REs deployed in RS s is constrained by its TPC, i.e., $N_s = P_s^{\max} - \zeta_s^{-1}P_{r,s}/\left(P_{\text{PS}} + P_{\text{DC}}\right)$ or $N_s = P_s^{\max} - \zeta_s^{-1}P_{r,s} - L_sP_{\text{DC}}/P_{\text{PS}}$ for an FC- or SC-active RS, respectively. When RS1 is active and RS2 is passive, then assuming a total deployment budget W_0, the number of passive REs is constrained as $N_2 = \frac{W_0 - P_1}{P_{\text{PS}}}$.

D. Complexity Analysis

The proposed joint TP/RB schemes are summarized in the BCA Algs. 1 and 2. The computational complexity of solving a standard convex QCQP having m variables and n constraints with an accuracy tolerance ε is given by $\mathcal{O}\left(\log_2(1/\varepsilon)\sqrt{m+n}(1+m)m^3\right)$. In (P3) and (P7), $m = MK$ and $n = 2$ or $n = 3$, respectively, while in (P4-A) and (P8-A), $m = N_1$ and $n = 1$. Likewise, in (P8-B), $m = N_2$ and $n = 1$. The combined complexity of (P3) and (P4-A) is given by $\mathcal{C}_1 = \mathcal{O}\left(\log_2(1/\varepsilon)\left(M^{4.5}K^{4.5} + N_1^{4.5}\right)\right)$ [8]. The computational complexity of the MM algorithm is given by $\mathcal{C}_2 = \mathcal{O}\left(N_2^3 + I_{MM}N_2^2\right)$, where I_{MM} denotes the number of iterations required for converge [13]. The complexity of updating $\boldsymbol{\mu}$ and $\boldsymbol{\mu}'$ is $\mathcal{O}\left(KM\right)$, whereas that of updating $\boldsymbol{\nu}$ and $\boldsymbol{\nu}'$ is $\mathcal{O}\left(K^2M + KN_1\right)$ and $\mathcal{O}\left(K^2M + KN\right)$, respectively [8]. Therefore, the overall complexity of Algs. 1 and 2 is respectively given by $\mathcal{O}\left(I_0\max\left\{\mathcal{C}_1, \mathcal{C}_2\right\}\right)$ and $\mathcal{O}\left(\log_2(1/\varepsilon)I_0'\left(M^{4.5}K^{4.5} + N_1^{4.5} + N_2^{4.5}\right)\right)$, where I_0, I_0' denote the number of iterations required for convergence.

IV. Numerical Evaluations

In this section, we evaluate the EE and SR of the considered hybrid RIS designs against the one achieved by benchmarks (namely, the fundamental RIS architectures and equivalent double RIS setups) via numerical simulations. We assume $N = 64$, $M = 4$, $K = 2$, $W_{\text{BS}} = 6$ dBW, $W_{\text{UE}} = W_{\text{PS}} = W_{\text{DC}} = 10$ dBm, $P_{\text{BS}}^{\max} = P_s^{\max} = 9$ dBW, $\xi = \zeta_s = 0.909$, and $\sigma_k^2 = \delta_s^2 = -80$ dBm, $\forall s \in \mathcal{S}$, $\forall k \in \mathcal{K}$. Rician fading channels with Rician factor $\kappa = 5$ dB and path loss exponent $\alpha_{\text{PL}} = 2.2$ are considered. The BS and RIS coordinates are $(0\text{m},\ -20\text{m},\ 0\text{m})$ and $(100\text{m},\ 5\text{m},\ 0\text{m})$, respectively.

Algorithm 1 BCA Algorithm for Solving (P2).

1: Randomly initialize $\mathbf{w}$ and $\boldsymbol{\phi}_s$, $s \in \mathcal{S}$; set $j = 0$.
2: **repeat**
3: Update $\boldsymbol{\mu}$ and $\boldsymbol{\nu}$ via Eq. (15).
4: Update $\mathbf{w}$ via Eq. (19).
5: Update $\boldsymbol{\phi}_1$ via Eq. (22).
6: Update $\boldsymbol{\phi}_2$ via Eq. (27).
7: $j \leftarrow j + 1$
8: **until** Convergence.
9: **Output:** $\{\mathbf{w}^\star, \boldsymbol{\phi}_s^\star\}$.

Algorithm 2 BCA Algorithm for Solving (P6).

1: Randomly initialize $\mathbf{w}$ and $\boldsymbol{\phi}_s$, $s \in \mathcal{S}$; set $j = 0$.
2: **repeat**
3: Update $\boldsymbol{\mu}'$ and $\boldsymbol{\nu}'$ via Eq. (30).
4: Update $\mathbf{w}$ via Eq. (34).
5: Update $\boldsymbol{\phi}_s$ via Eq. (37).
6: $j \leftarrow j + 1$
7: **until** Convergence.
8: **Output:** $\{\mathbf{w}^\star, \boldsymbol{\phi}_s^\star\}$.

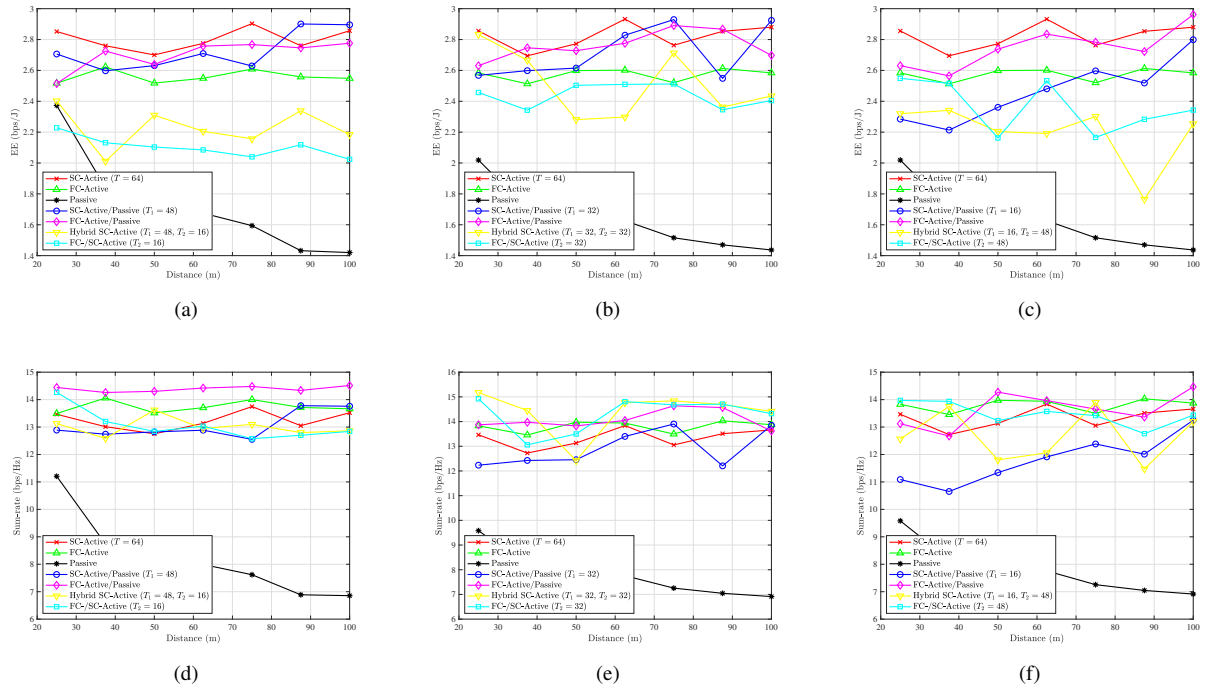

Fig. 3. EE (top) and SR (bottom) vs. user position for $\{N_1, N_2\} = \{\{48, 16\}, \{32, 32\}, \{16, 48\}\}$ ({left},{center},{right}) and $L_s = 1$.

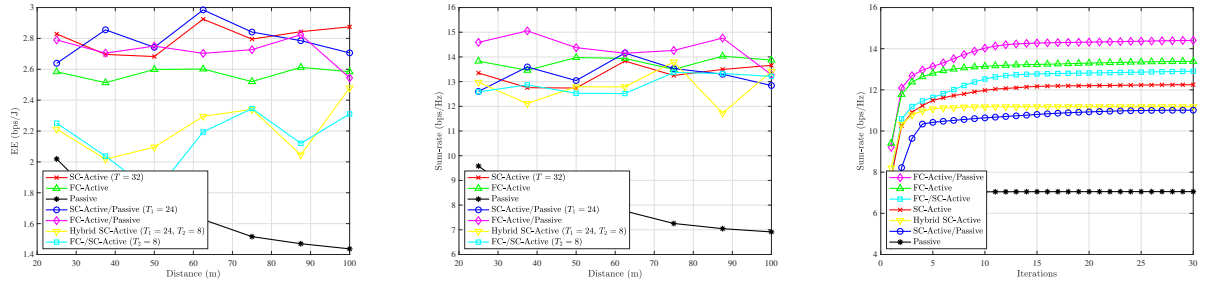

Fig. 4. EE (left) and SR (center) vs. user position for $\{N_1, N_2\} = \{\{48, 16\}\}$ and $L_s = 2$. SR vs. iterations (right).

In Figs. 3 and 4, the users move together along the x axis. We plot the performance vs. the distance of the user cluster from the BS for various hybrid RIS configurations. We observe the following: The proposed SC-active/passive design achieves the highest EE with moderate/high number of active REs at moderate/high distances, since then the combination of a single PA and passive RB is effective. SC-active RIS achieves the best EE in all other cases, thanks to its small TPC. Passive RIS has the worst EE and SR performance, due to the product path loss. FC-active/passive RIS's EE improves by reducing the number of active REs, since we reach a favorable amplification gain/noise balance, but worsens with an excessive number of passive REs unless the users are located near the RIS where amplification is effective. Active/passive designs have better EE than the FC-active RIS, due to their fewer PAs and sufficient SR. Hybrid SC-active and FC-active/SC-active designs significantly outperform passive RIS in terms of EE. Their EE is benefiting from moderate/small number of SC-/FC-active REs, such that the SR/TPC is sufficiently high/low, respectively. FC-active/passive RIS presents the best SR with high number of active REs. SC-active/passive RIS's SR drops as the number of passive REs increases, since then a single PA is not effective. Hybrid active and SC-active designs outperform SC-active/passive RIS in SR, due to the product path loss. Using smaller partitions improves SC-active/passive RIS's EE, due to the enhanced SR that overcomes the slight TPC increase, and hybrid active designs' EE and SR. Lastly, on the right column of Fig. 4 we plot the achieved SR vs. the number of iterations. We note that the developed algorithms converge quickly in practice.

In Fig. 5, the users are placed on moderate distance from the BS. On the left column, we vary the TPC budget of the

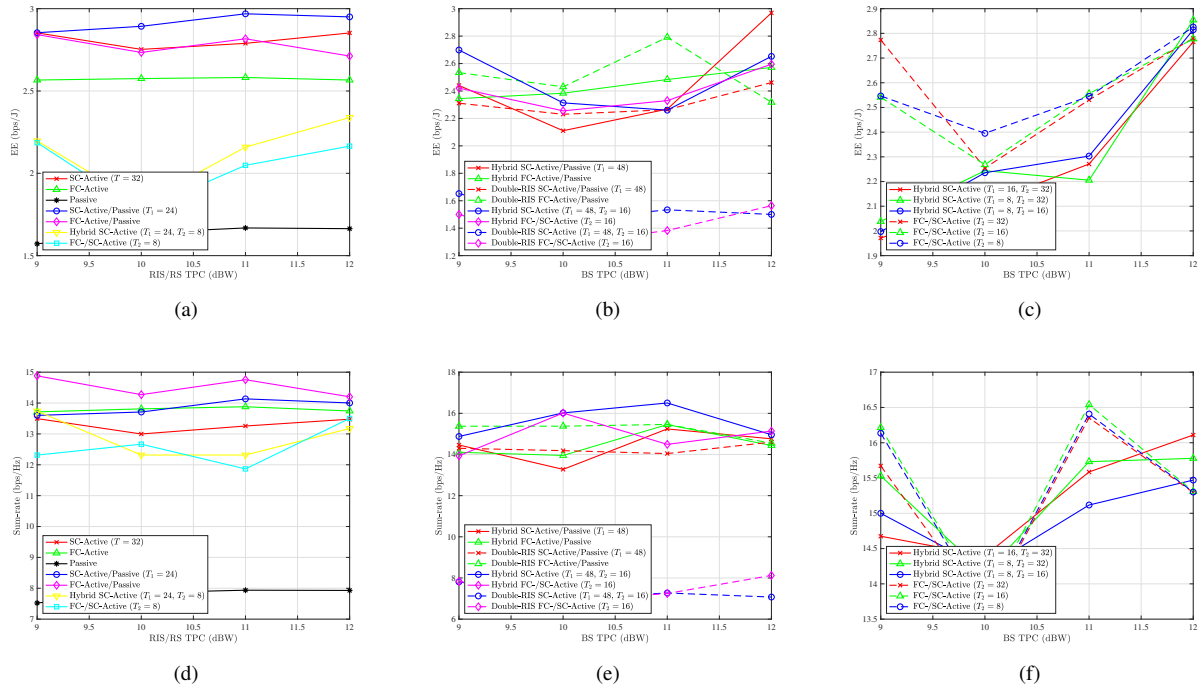

(a) (b) (c)

(d) (e) (f)

Fig. 5. EE (top) and SR (bottom) vs. active RIS/RS(s) TPC budget (left), BS TPC budget (center), and number of partitions (right). We have $\{N_1, N_2\} = \{48, 16\}$ on the left and center columns with $L_s = 2$ or $L_s = 1$, respectively, and $\{N_1, N_2\} = \{32, 32\}$ on the right column.

active RIS/RS(s). We observe the following: The performance of hybrid structures that employ the SC-active design improves with higher budget, while that of hybrid RISs that adopt the FC-active architecture faces diminishing returns due to the amplification noise. On the center and right columns, we vary BS's TPC budget. we notice that the hybrid SC-active/passive RIS achieves the highest EE for high budget, while the double FC-active/passive RIS setup presents the best performance in all other scenarios due to the RIS placement. The other double RIS setups present the worst EE and SR performance for the same reason. The hybrid active RIS designs achieve the highest SR. A moderate partitioning boosts SR, while larger/smaller partitions benefit EE for smaller/larger budget, respectively.

V. Conclusions

In this work, we introduced novel hybrid RIS architectures with high flexibility in striking a desirable SR/TPC balance and proposed joint TP/RB designs that maximize the EE. Numerical simulations unveiled their performance gains over benchmarks and their favorable operational regimes. In the future, we plan to optimize REs' allocation and develop robust schemes against channel uncertainty.

References

[1] G. Zhou, C. Pan, H. Ren, K. Wang, and A. Nallanathan, "A Framework of Robust Transmission Design for IRS-Aided MISO Communications With Imperfect Cascaded Channels," *IEEE Trans. Signal Process.*, vol. 68, pp. 5092–5106, Aug. 2020.

[2] X. Yu, D. Xu, D. W. K. Ng, and R. Schober, "IRS-Assisted Green Communication Systems: Provable Convergence and Robust Optimization," *IEEE Trans. Commun.*, vol. 69, no. 9, pp. 6313–6329, Sep. 2021.

[3] H. Guo, Y.-C. Liang, J. Chen, and E. G. Larsson, "Weighted Sum-Rate Maximization for Intelligent Reflecting Surface Enhanced Wireless Networks," in *IEEE Global Commun. Conf. (GLOBECOM)*, Waikoloa, HI, USA, Dec. 2019.

[4] C. Huang, A. Zappone, G. C. Alexandropoulos, M. Debbah, and C. Yuen, "Reconfigurable Intelligent Surfaces for Energy Efficiency in Wireless Communication," *IEEE Trans. Wireless Commun.*, vol. 18, no. 8, pp. 4157–4170, Aug. 2019.

[5] K. Zhi, C. Pan, H. Ren, K. K. Chai, and M. Elkashlan, "Active RIS Versus Passive RIS: Which is Superior With the Same Power Budget?" *IEEE Commun. Lett.*, vol. 26, no. 5, pp. 1150–1154, May 2022.

[6] R. Long, Y. Liang, Y. Pei, and E. G. Larsson, "Active Reconfigurable Intelligent Surface Aided Wireless Communications," *IEEE Trans. Wireless Commun.*, vol. 20, no. 8, pp. 4962–4975, Aug. 2021.

[7] D. Xu, X. Yu, D. W. Kwan Ng, and R. Schober, "Resource Allocation for Active IRS-Assisted Multiuser Communication Systems," in *Asilomar Conf. Signals, Syst., Comput.*, 2021, pp. 113–119.

[8] Z. Zhang *et al.*, "Active RIS vs. Passive RIS: Which Will Prevail in 6G?" *IEEE Trans. Commun.*, 2023, Early Access.

[9] K. Liu, Z. Zhang, L. Dai, C. Xu, and F. Yang, "Active Reconfigurable Intelligent Surface: Fully-Connected or Sub-Connected?" *IEEE Commun. Lett.*, vol. 26, no. 1, pp. 167–171, Jan. 2022.

[10] Z. Kang, C. You, and R. Zhang. (2022, Jul.) Active-Passive IRS aided Wireless Communication: New Hybrid Architecture and Elements Allocation Optimization. arXiv preprint. [Online]. Available: https://arxiv.org/pdf/2207.01244.pdf

[11] A European Green Deal: Striving to be the first climate-neutral continent. Online. [Online]. Available: https://commission.europa.eu/strategy-and-policy/priorities-2019-2024/european-green-deal_en

[12] K. Shen and W. Yu, "Fractional Programming for Communication Systems—Part I: Power Control and Beamforming," *IEEE Trans. Signal Process.*, vol. 66, no. 10, pp. 2616–2630, May 2018.

[13] X. He and j. Wang, "QCQP With Extra Constant Modulus Constraints: Theory and Application to SINR Constrained Mmwave Hybrid Beamforming," *IEEE Trans. Signal Process.*, vol. 70, pp. 5237–5250, Oct. 2022.